COSY Beam Time Request

For Lab. use

Exp. No.:	Session No.
E 00?.?	**11**

Collaboration: **JEDI**

Optimization of the alignment of magnetic elements using the spin tune response to three-steerer bumps

Jülich, 09.12.2019

Spokespersons for the beam time:

Artem Saleev (Jülich)
Vera Shmakova (Jülich)
Paolo Lenisa (Ferrara)
Frank Rathmann (Jülich)

Spokespersons for the collaboration:

Paolo Lenisa (Ferrara)
Jörg Pretz (Aachen/Jülich)

Address:
Institut für Kernphysik
Forschungszentrum Jülich
52428 Jülich
Germany

Phone: **+49 2461 61 5884** Fax: **+49 2461 61 3930**

E-mail:
a.saleev@fz-juelich.de
v.shmakova@fz-juelich.de
f.rathmann@fz-juelich.de

lenisa@fe.infn.it
pretz@physik.rwth-aachen.de

Total number of particles and type of beam (p, d, polarization)	Kinetic energy (MeV)	Intensity or internal reaction rate (particles per second) minimum needed	Intensity or internal reaction rate (particles per second) maximum useful
Polarized deuterons	**~970 MeV/c**	**stored ~10^9**	**stored ~10^{10}**
Experimental area	Safety aspects (if any)	Earliest date of Installation	Total beam time (No. of shifts)
WASA detector, electron cooler, RF solenoid, Siberian snake, orbit correction, sextupoles	**None**	**August 15, 2020**	**2 MD + 3 weeks**

Optimization of the alignment of magnetic elements using the spin tune response to three-steerer bumps

A. Saleev, P. Lenisa, F. Rathmann, V. Shmakova and J. Pretz

December 10, 2019

Abstract

Searches of electric dipole moments (EDM) of charged particles in pure magnetic rings, such as COSY, or electrostatic and hybrid magnetic-electric storage rings, planned in the future, require new methods to disentangle the EDM signal from the large background produced by magnetic dipole moments. In the JEDI precursory experiment, the sources of systematic background are non-ideal magnetic element alignments that lead to in-plane imperfection magnetic fields. Spin tune mapping is a novel tool to probe the spin dynamics in a storage ring and we propose to use it together with a new method where the spin tune is shifted by applying a vertical three-steerer closed-orbit bump. At COSY there are many options where to create such vertical bumps. That allows us to determine the local properties of the imperfection fields and to optimize the magnetic element alignment and setting in the machine.

1 Introduction

The electric dipole moment (EDM) signal constitutes a rotation of the spin in the electric field. In an all magnetic ring (COSY), it is the motional electric field $\propto [\vec{\beta} \times \vec{B}]$ along the radial x-axis around which the EDM precesses. As such, an EDM contributes also to a constant tilt of the stable spin axis

$$\vec{c} = \vec{e}_y + \xi_{\text{edm}} \vec{e}_x \tag{1}$$

On the other hand, nonuniform in-plane imperfection magnetic fields tilt the invariant spin axis towards x or z (see Fig. 1),

$$\vec{c} = c_y \vec{e}_y + (\xi_{\text{edm}} + c_x^{\text{mdm}})\vec{e}_x + c_z^{\text{mdm}}\vec{e}_z. \tag{2}$$

While $c_y \simeq 1$, the projections $c_{x,z}$ depend on the specific location chosen to define the one-turn spin transfer matrix. In the example shown in Fig. 2, the vertical closed orbit of the reference particle is perturbed by the imperfection transverse field of the tilted dipole BE7, in the otherwise ideal COSY ring (simulations results obtained using COSY-Infinity[2]). Spin rotations in the radial focusing fields of the quadrupoles that keep the particle on the closed orbit are non-commuting with the spin rotations around the vertical field of the dipoles. Imagine a position-dependent polarimeter to observe polarisation rotation in some location in the ring. The order of the spin rotations in the dipoles and quadrupoles after one turn of the particle over the ring will be different for different locations of the observation point, thus the resulting axis $\vec{c}$ of the one-turn spin transfer matrix will also be different (see also discussion in ref.[1] Chap.2 Sec.IV).

Simulations of the spin dynamics for the orbit shown in Fig. 2 allow us to calculate the directions of $\vec{c}$ when the starting point is selected behind each dipole, MQU-family quadrupole and vertical steerer, and results for the projections c_x and c_z are shown in Fig. 3 (black curves for both c_x and c_z). One must bear in mind that in the general case, the stable spin axis is an integral property of the ring, and c_x receives contributions from the local longitudinal imperfection fields as well, and vice versa, c_z receives contributions from the local radial imperfection fields.

Unlike $c_{x,z}^{\text{mdm}}$, the EDM contribution to $\vec{c}$ is *invariant* along the orbit. The red, green and blue curves in Fig. 3 represent the simulations with the same settings as in those used for the black curves, but with different assumptions about the size of the non-vanishing EDM. For the c_x components, one can see a parallel shift of the curves with respect to increasing EDM, which is in agreement with analytical expectation based on Eq. (2).

It is not possible to move the observation point (a polarimeter) to a desired location in the ring. But, as it was demonstrated in [4], it is possible to create a spin kicks by the solenoids at certain locations of the ring and observe the change of the spin tune – the quantity that does not depend on the location of the observation point – to determine the projection c_z of the invariant spin axis at the location of the solenoids.

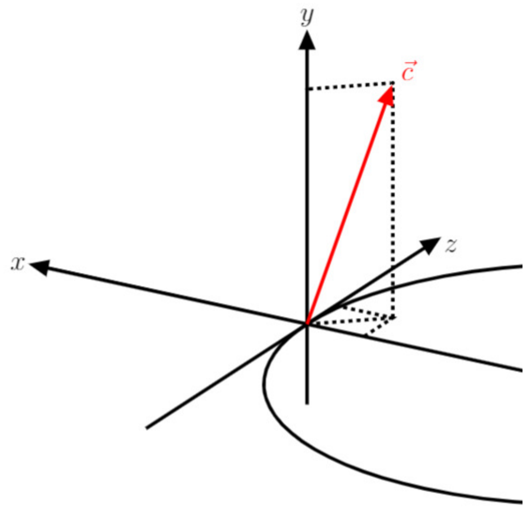

Figure 1: Sketch of the components of the invariant spin axis $\vec{c}$ at some point along the closed orbit trajectory.

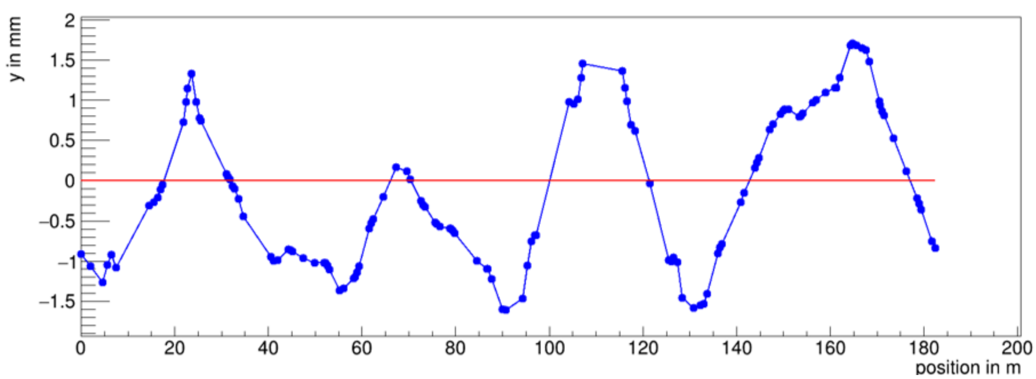

Figure 2: Vertical (blue) and horizontal (red) closed orbit for reference particle (deuterons at P=970 MeV/c). The imperfection is generated by the rotation of the dipole $BE7$ around z-axis by 1 mrad.

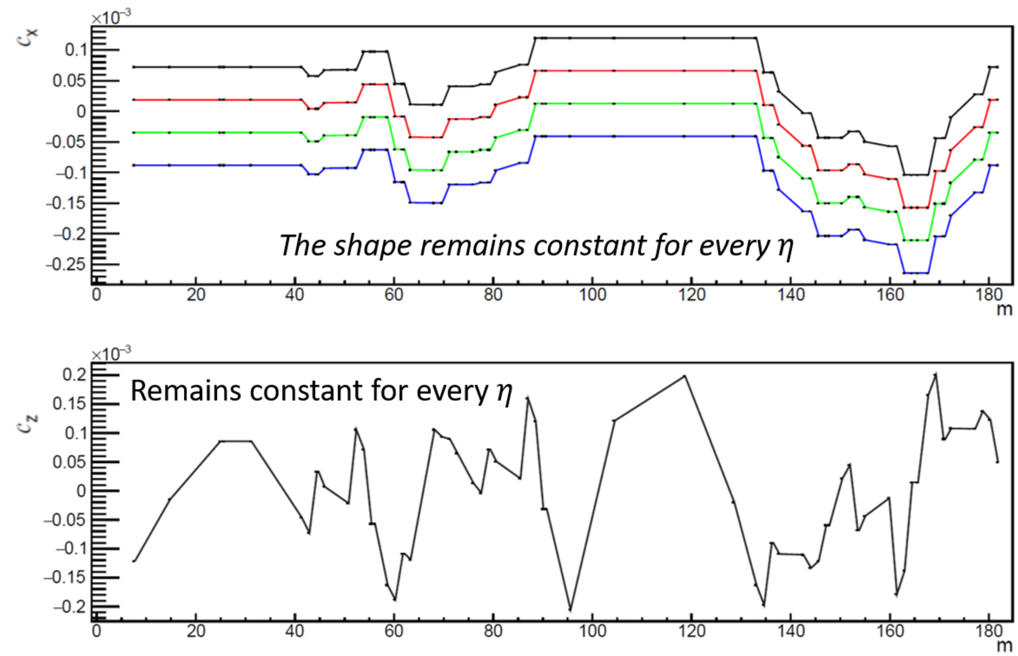

Figure 3: Variation of imperfection components of the invariant spin axis $\vec{c}$ calculated at the positions of the ring elements, as given by simulations using COSY-Infinity[2], for the closed orbit shown at Fig.3. The color code represents different values of η-factor, here the EDM d is parametrized as $d = \eta\frac{q\hbar}{2mc}$, starting from zero (black curve) increasing to 10^{-4} (blue curve). The red and green curves are for $\eta = 0.33 \cdot 10^{-4}$ and $\eta = 0.66 \cdot 10^{-4}$ respectively. The EDM does not contribute to the c_z projections, and thus the curve for c_z remains the same for all simulations with different η.

The quantitative understanding of the local sources of the imperfection fields and their active compensation is indispensable for disentangling the EDM effect from the EDM-like background from interactions of the vastly larger magnetic dipole moment with the in-plane magnetic fields. This proposal aims at probing the local imperfection properties of the COSY ring. Optimization of the imperfection properties of COSY will provide invaluable additional information for the interpretation of the results of the forthcoming JEDI precursor experiment of the deuteron EDM.

2 Effect of the bump on the spin tune

The spin tune denotes the number of spin rotations in one turn of a particle in the ring. It can be determined to a very high precision, with a relative error of 10^{-10} during a 100 s long beam cycle [3]. Such precision allowed us to develop a new method, called "spin tune mapping" [4]. It is based on the measurement of the spin tune shift with respect to different artificial imperfection fields created in the ring. The spin tune shifts can be predicted by a model and then the model parameters can be determined. Experimentally, in the new approach, proposed here, we suggest to use steerer fields (assuming the role of those artificial imperfection fields) in a predictable manner, namely creating local vertical closed orbit bumps.

The bumps are produced by three consecutive vertical steerers (see Fig. 4). In order to keep the bump a closed one at all magnitudes of the bump, the steerer kicks must be kept proportional to each other. The proportionality coefficients would depend on the betatron phase advances and beta functions in the steerers. The maximum orbit perturbation created by any bump in the simulations is assumed to be 15 mm, the amplitudes of steerer kicks for different bumps are adjusted accordingly. The relative orbit shift (excluding the part of the orbit with the bump itself) when the bump steerers are switched on should be less than 0.2 mm at this amplitude. The spin rotation in the bump is predicted by spin tracking using COSY-Infinity [2]. It is similar to that caused by a weak helical snake. Effectively, it produces a spin kick around a fixed in-plane axis $\vec{w} = \vec{e}_x \sin\alpha + \vec{e}_z \cos\alpha$, where α is a directional angle that is counted from the positive axis z towards the positive axis x (see Fig. 5). The magnitude of the spin kick ψ in the bump is proportional to the steerer kick angle θ of a central steerer in the bump which is chosen as a reference one. The bump amplitude is also proportional to θ.

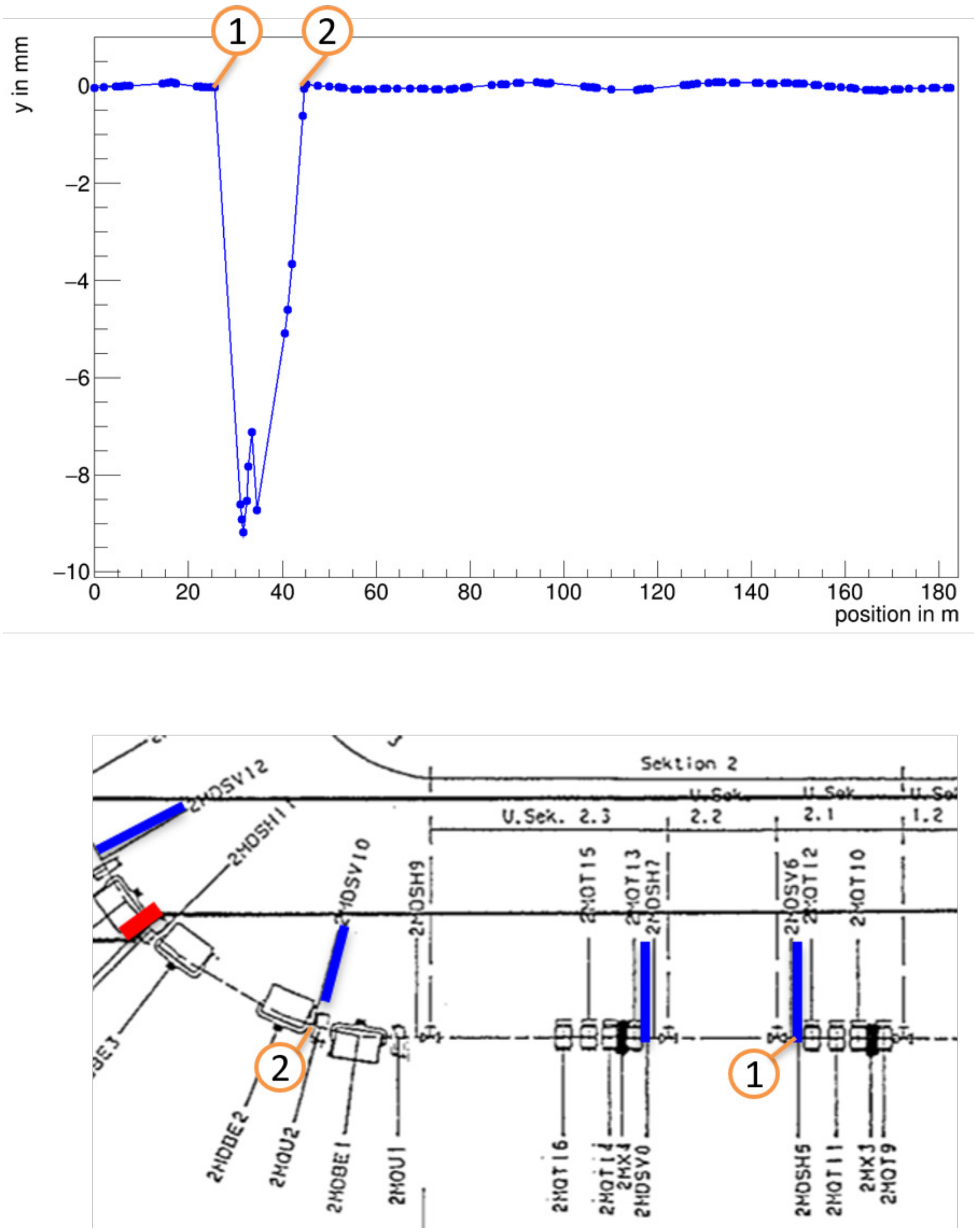

Figure 4: Example of the bump with steerers MSV 6 - 8 - 10 (marked with blue lines).

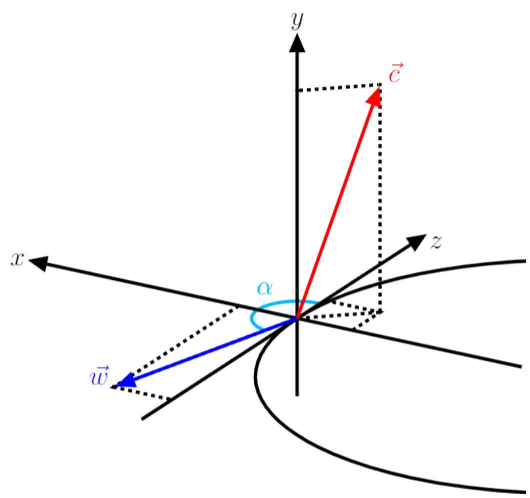

Figure 5: Relative orientation of vectors $\vec{c}$ and $\vec{w}$.

Both analytic and lattice models predict that the spin tune has a parabolic dependence on the bump amplitude (see Fig. 6). The corresponding analytic result is

$$\cos\pi(\nu_s + \Delta\nu_s) = \cos\pi\nu_s \cos\frac{\psi}{2} - (\vec{c}\cdot\vec{w})\sin\pi\nu_s \sin\frac{\psi}{2} \tag{3}$$

where $(\vec{c}\cdot\vec{w}) = c_x \sin\alpha - c_z \cos\alpha$ defines the offset of the minimum of a parabola. The components of the invariant spin axis c_x and c_z are defined after the last steerer of the bump. The parameter α is specific for each bump, the COSY-Infinity simulations suggest clustering around $\sim -40^\circ$ or $\sim -65^\circ$. Here we mention that the method is not sensitive to the in-plane projection of the invariant spin axis $\vec{c}$ should it be orthogonal to $\vec{w}$ of a particular bump.

However, in the experiment it is not possible to resolve c_x and c_z separately. In the measured spin tune shifts produced by the bump, there are only two parameters used in the analytic model: the parabolic curvature and the location of the minimum controlled by by the cosine of the opening angle between $\vec{c}$ and $\vec{w}$,

$$(\vec{c}\cdot\vec{w}) = \cos\angle(\vec{c},\vec{w}) \ = -\sin\zeta. \tag{4}$$

The angle ζ specifies by how much $\angle(\vec{c},\vec{w})$ deviates from $\pi/2$. The error on ζ depends on the number of measurements, the maximum attainable ψ, and the systematical (as well as statistical) error of the spin tune shifts which depend

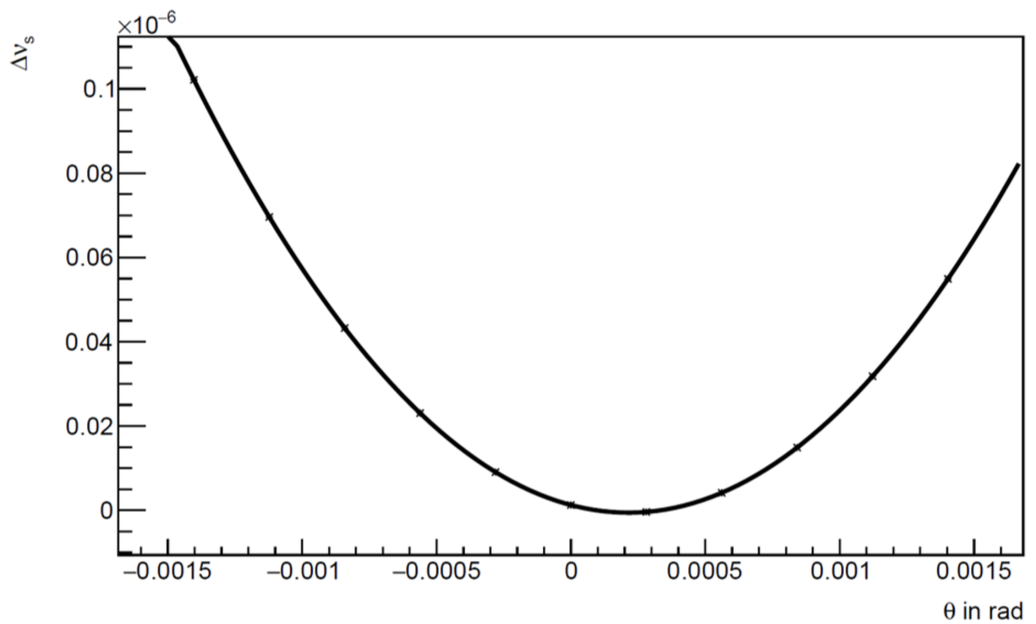

Figure 6: A model prediction of the spin tune shifts for the bump MSV 8 - 10 - 12 with respect to the kick angle θ of the central steerer (COSY-Infinity simulation with COSY lattice). The minimum is shifted by the imperfection solenoid field of 0.5 Tmm in the second straight section (see Fig.9).

on the cycle length. The typical error of ζ, assuming the same parameters as in [4], is of the order of $\sigma_\zeta \approx 10^{-6}$ rad. The fit of the measured spin tune shifts can be also performed directly in COSY-Infinity [2]. In this case, the lattice parameters, namely the element alignments, are optimized with χ^2-minimization. Such fits should be rather performed on the measured spin tune maps from all of the bumps simultaneously.

It is important that the bumps are as closed as possible, i.e., are causing the least possible perturbation of the orbit except in the bump itself. If the relative orbit shift in the ring when the bump steerers are switched on is larger than 0.2 mm, it will have an impact on the location of the minimum and will increase the systematic error at its location. Orbit shifts higher than 0.4 mm will significantly reduce the spin coherence time (SCT), because the orbit in the sextupoles is not optimal anymore for a correction of the chromaticity.

3 Spin tune maps with bumps and solenoid

A superconducting solenoid (see Fig.9), the same as to be used in the precursor experiment, should be used in conjunction with each bump. The bump steerers and the solenoid should be switched on and off simultaneously within a single beam cycle (see Fig.7). The spin tune shift $\Delta\nu_s$ that corresponds to the central flattop in Fig.7 will have a dependence on the crosstalk between solenoid and bump, given by:

$$\begin{aligned} \cos\pi(\nu_s + \Delta\nu_s) \quad = \quad & \cos\pi\nu_s \cos\frac{\psi}{2}\cos\frac{\chi}{2} \\ & -(\vec{c}^{\,\mathrm{bump}}\cdot\vec{w})\sin\pi\nu_s\sin\frac{\psi}{2}\cos\frac{\chi}{2} \\ & -(\vec{c}^{\,\mathrm{sol}}\cdot\vec{e}_z)\sin\pi\nu_s\cos\frac{\psi}{2}\sin\frac{\chi}{2} \\ & -\cos(\alpha-\Delta\theta)\sin\frac{\psi}{2}\sin\frac{\chi}{2}, \end{aligned} \tag{5}$$

where $\Delta\theta$ denotes the difference of the spin phase advance calculated from the spin transfer matrices between solenoid and last steerer of the bump[1]. Unknown vectors $\vec{c}^{\,\mathrm{sol}}$ and $\vec{c}^{\,\mathrm{bump}}$ define the directions of the corresponding invariant spin axes at the locations of the solenoid and last steerer of the bump. The last term is $\propto \sin\frac{\psi}{2}\sin\frac{\chi}{2}$ which means that $\cos(\alpha-\Delta\theta)$ has an impact on the parabolic curvature and the parameter α can be determined independently from the imperfections present in the ring. This means the solenoid acts as a benchmark for every bump, providing access to the directional angle α which can be compared to the model prediction of the bump. An example of the spin tune map with bump MSV 8 - 10 - 12 and solenoid is given in Fig. 8.

4 Estimate of the required beam time

The use of solenoid also would allow us to boost the spin tune shifts above the spin tune drift and cycle variations threshold of $\delta\nu_s \sim 10^{-8}$ (see [4]). Each measurement of the spin tune map with solenoid and bump should

[1]Approximately given by how many more dipoles are present counting in counterclockwise direction to the bump from the solenoid from that counting in clockwise, times $2\pi\nu_s$

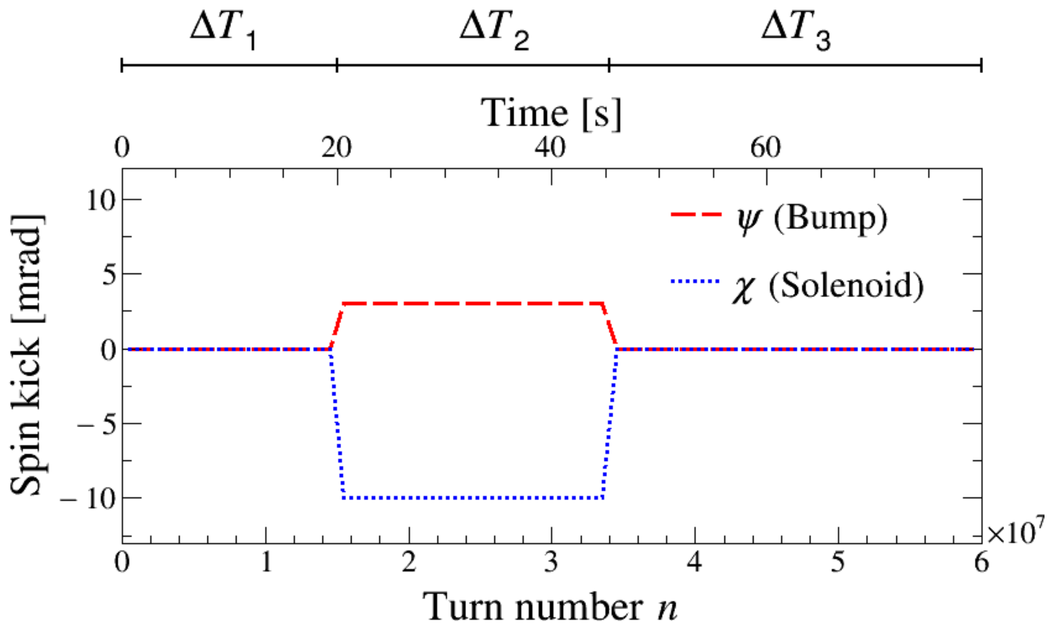

Figure 7: A scheme for switching on and off the bump and solenoid. The times ΔT_1, and ΔT_3 denote when the bump steerers and solenoid are switched off, and during the time ΔT_2 the bump steerers and solenoid are simultaneously switched on with constant currents.

take roughly 24 hours. If 200 second long cycles are assumed, this allows us to take a mesh of 9 by 9 points with 4 cycles in each setting, which amount to 18 hours of continuous measurement. Another advantage of using the solenoid is that the sensitivity to the spin tune shift within one cycle is also increased, as there is no need to do many flattops with different bumps in a single cycle.

Measurements of the vertical asymmetry to determine the spin tune from the rapidly precessing horizontal polarization have been routinely carried out using the WASA for the precursor and the JEDI experiment, the same status regarding the superconducting snake solenoid is applicable.

The overall requirements for the measurement for a sufficient number of maps are

- 2 days: setup of working point with long spin coherence time for a particular bump (for all amplitudes of the bump)

- 1 day: spin tune mapping for this bump with solenoid (as shown in

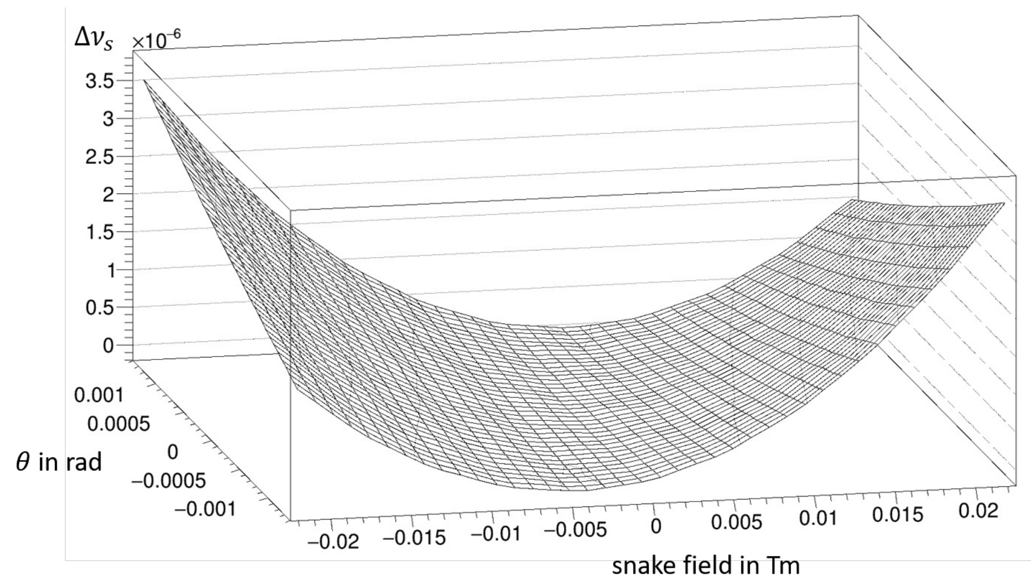

Figure 8: Spin tune map of COSY with the bump MSV 8 -10 - 12 and superconducting solenoid. The surface connects the points from the simulation using COSY-Infinity.

Figs. 7 and 8)

- at least 7 different spin tune maps should be measured with different steerers to create bumps (see Table 1 for the anticipated steerer configurations)

This yields a total amount of 21 days = 3 weeks to accomplish the goals of this proposal. During 2 machine development weeks all of the bumps should be tested and matched. The maximal attainable amplitudes of the bumps should be determined. The criteria to select the maximal amplitude is such that the maximum additional orbit perturbation in the ring except of the bump itself should be less than 0.2 mm.

Some bumps can have much smaller maximal amplitudes than the others. For that reason, to achieve the same statistical sensitivity for the parameter $\zeta \simeq -(\vec{c}^{\,\text{bump}} \cdot \vec{w})$ of $\sigma_\zeta \simeq 10^{-6}$ rad, the cycle length should be adjusted for each bump configuration (see Table 1) individually. Of course, the measurement of the spin tune map for such bump could take longer than one day, but should be no more then two days. If the maximal amplitude of the bump appears to be less than 5 mm, it should not be used for the spin tune mapping.

5 Roadmap to the precursor experiment

After the alignment survey and field probe measurements, the direction of the invariant spin axis at any location of the ring can be predicted by spin dynamics simulations on the closed orbit [5]. The limit on the EDM is determined from the difference of the predicted and measured x-projection of the invariant spin axis.

A minimization procedure to fit the element alignments and settings to the measured spin tune maps for all bumps should be developed. Following the standard routines, the orbit response matrix (ORM) can be used to generate a proper COSY model (especially the settings of $k1$-values for quadrupoles) as a guidance to provide an initial approximation to search for the minima (and vice versa). The simulations of the orbit perturbation by the bumps should be in line with those of the ORM. The responce to bumps would allow to disentangle at least partially the relative significance of the quadrupole offsets and dipole misalignments.

The EDM can be implemented as a free parameter, it is an equal increment of c_x for any model assumtion of $\vec{c}$ all around in the ring. The estimated sensitivity is at least $d = 10^{-19}$ e·cm and higher.

The present proposal has two goals:

1. It complements the precursor experiment on the first direct deuteron EDM measurement with RF Wien filter with additional measurements of the direction of the spin precession axis $\vec{c}$ at different locations (although components c_x and c_z can not be resolved separately), and

2. It indicates the applicability of the magnetic element alignment by a quantitative description of how uniform the axis $\vec{c}$ is from one location to another in the ring

6 Systematic errors of the method

When the bump is not closed, the orbit perturbations in the ring modify $\vec{c}^{\,\text{bump}}$ and the base spin tune ν_s that were assumed to be constant for any bump amplitude. The same is also true for $\vec{c}^{\,\text{sol}}$ at the solenoid if the misalignment of the beam with respect to the optical axis of the solenoid makes it not transparent to the direction of the beam momentum. This leads to scaling effects of the spin kicks ψ and χ, which might complicate the interpretation of the resulting fit parameters. For that reason, the orbit deviations outside of the bump should be monitored online during the measurement, and these should not exceed 0.2 mm. A significant reduction of the spin coherence time or the inability to resolve the spin tune from the online data analysis at the end of beam cycle are other indications of orbit perturbations. Slow drift of the orbit during the day can also lead to such effects which means the reference orbit (when all bump steerers and solenoid are switched off) should be also tracked approximately once per hour.

The errors of the COSY model which depend on the correct settings of the quadrupoles ($k1$-values) should be minimized with the help of ORM measurement. It is important for the later interpretation of the parameter $\cos(\alpha - \Delta\theta)$ in Eq. (5) and the comparison of the directional angle α to the one assumed in the model. It could be useful to keep track of the parameters of orbit response matrix especially before the start of data taking (during the MD week), in the middle of the beam time and at the end. S sufficiently large number of measurements for the ORM could take a few hours.

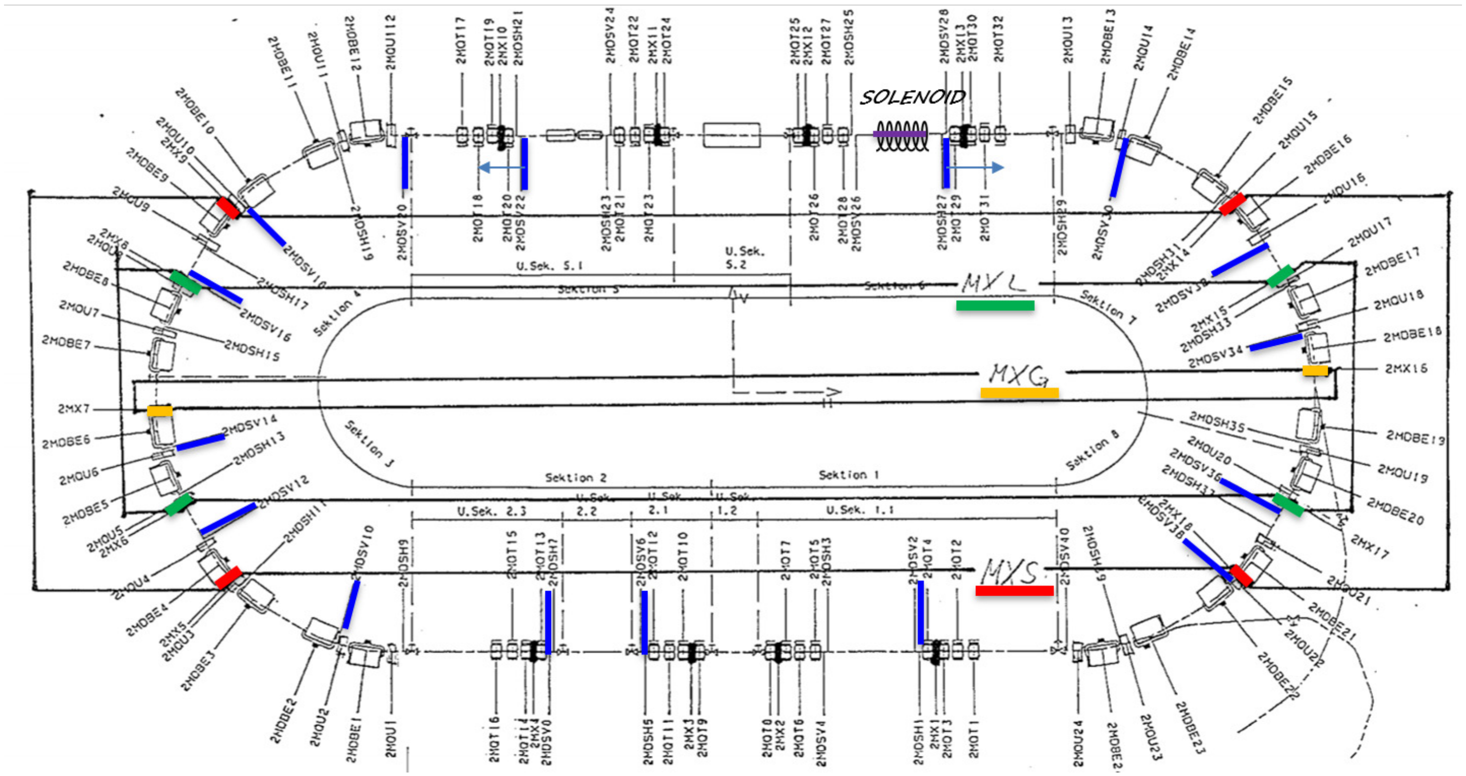

Figure 9: Scheme of COSY with vertical steerers marked as blue lines. Solenoid position is to the right from the center of the telescope, in section 6. Sextupoles of different families are also marked with MXS-red, MXG-orange, MXL-green lines. Black lines that connect those sextupoles represent the order of power lines.

The spin tune shifts related to the spin tune drifts within the cycle and from cycle to cycle are also major indicators of the unwanted changes in the machine setup. Variations of the spin tune ν_s (defined for reference orbit when bump steerers and solenoid are switched off) by $\delta\nu_s \approx 10^{-8}$ from cycle to cycle are considered to be normal, as depicted in Fig.4 of Ref. [3]. Spin tune drifts over 80 seconds of the beam cycle with RMS value for all cycles $3.2 \cdot 10^{-9}$ were considered as the main source of systematic errors for the spin tune shifts $\Delta\nu_s$ in [4], and we expect the same or smaller errors in the experiment proposed here.

7 Chromaticity correction

To set up the high precision spin tune measurement, a long spin coherence time of the order of a few hundred seconds is needed. Usually the sextupoles are set up such that vertical and horizontal chromaticities simultaneously vanish [6]. Fine tuning the sextupoles of the MXS and MXG families, one determines the location, where the spin coherence time reaches the optimum. The greatest hurdle of the proposed experiment is that when the vertical orbit bump is set up, the vertical orbit shift in the sextupoles located within the bump will significantly change the chromaticity and detune the machine setup from the optimum.

For that reason, those particular sextupoles within the bump have to be switched off during the spin tune mapping. The list of the bump configurations using three MSV steerers, the corresponding amplitudes of central steerer kicks θ (at which the bump displacement is 15 mm) and the sextupoles that should be switched off are given in table 1 (see also Fig. 9 for the location of steerers and sextupoles). The technical ability to disconnect a single sextupole from family should be developed and implemented during the summer shutdown. A first test of the procedure will be already carried out by the machine crew in January 2020, and sextupole power supplies will be tested to provide the required operation.

When a sextupole is removed from a family, the chromaticity should be adjusted with the remaining sextupoles. To facilitate the optimization of the remaining sextupoles for long SCT, a chromaticity measurement should be set up, based on the recently developed tool for fast betatron tune measurement. Once the chromaticity is mapped with respect to the sextupole strengths, the working point for sextupole settings where chromaticity equals

Steerer			Amplitude	Sextupoles inside bump, MX[n]		
MSV	MSV	MSV	θ [mrad]	MXS	MXL	MXG
6	8	10	1.3426			
8	10	12	1.4030	05		
10	12	14	1.9535	05	06	
12	14	16	5.1938		06, 08	07
14	16	18	2.0966	09	08	07
16	18	20	4.8600	09		
30	32	34	1.9487	14	15	
32	34	36	5.1411		15, 17	16
34	36	38	2.2081	18	17	16
36	38	2	3.9855	18		

Table 1: The bump configurations and sextupoles needed to be switched off (see also Fig. 9).

zero is selected, and fine scans for the best SCT can be performed. Simulations using COSY-Infinity are used to provide guidance for the correction. Such a procedure is anticipated to take no more than 2 to 3 days.

Electron cooling of the beam after injection is also required to reduce decoherence effects related to the momentum spread. But all ecooler magnets should be switched off during the data taking in the cycle, as is usually already done in the precursor experiment.

Fine adjustments of sextupoles for best SCT for every bump could be performed with a feedback system based on an automated chromaticity correction. The preparation of a reliable and precise tool for the chromaticity measurement is needed in the first half of the year 2020.

8 Beam request

The JEDI collaboration would like to request beam time to collect data of seven spin tune maps. As an outcome of the beam time we want to have a working tool for optimization of magnetic element alignments on the basis of the precision spin dynamics, which is important for JEDI precursor experiment at COSY and for future storage rings. The experiment needs longer setup times related to strict requirements to set up the bumps which is crucial for a smooth operation, and therefore **we request 2 weeks of machine development time and 3 weeks of measurement time**, to be tentatively scheduled at the end of the 3rd quarter 2020 (September).

References

[1] S. Y. Lee, Spin Dynamics and Snakes in Synchrotrons (World Scientific, 1997) `http://books.google.de/books?id=And2QgAACAAJ`

[2] Berz, M.: Computational aspects of optics design and simulation: COSY INFINITY. Nucl. Instrum. Meth. **A298**, 473–479 (1990). DOI 10.1016/0168-9002(90)90649-Q

[3] Eversmann, D., et al.: New method for a continuous determination of the spin tune in storage rings and implications for precision experiments. Phys. Rev. Lett. **115**, 094801 (2015). DOI 10.1103/PhysRevLett.115.094801

[4] Saleev, A., et al.: Spin tune mapping as a novel tool to probe the spin dynamics in storage rings. Phys. Rev. Accel. Beams **20**, 072801 (2017)

[5] Rathmann, F., Nikolaev, N.N., Slim, J.: Spin dynamics investigations for the EDM experiment at COSY `https://arxiv.org/pdf/1908.00350.pdf`.

[6] Guidoboni, G., et al.: Connection between zero chromaticity and long in-plane polarization lifetime in a magnetic storage ring. Phys. Rev. Accel. Beams **21**, 024201 (2018)